A paper resubmitted to Journal of Biomechanics

<Revised>

Estimation of the mechanical connection between apical stress fibers and the nucleus in vascular smooth muscle cells cultured on a substrate

Word count: 2799 from Introduction to Results and Discussion

Kazuaki NAGAYAMA, Sho YAMAZAKI,
Yuki YAHIRO, and Takeo MATSUMOTO

Biomechanics Laboratory, Department of Mechanical Engineering,
Nagoya Institute of Technology, Gokiso-cho, Showa-ku, Nagoya 466-8555, Japan

Mailing Address: Kazuaki Nagayama, Ph.D., Associate Professor
Takeo Matsumoto, Ph.D., Professor
Nagoya Institute of Technology *Omohi* College
Gokiso-cho, Showa-ku, Nagoya 466-8555, Japan
Tel/Fax: +81-52-735-5477 (KN), -5049 (TM)
E-mail: k-nagaym@nitech.ac.jp (KN)
takeo@nitech.ac.jp (TM)

Abstract

Actin stress fibers (SFs) generate intercellular tension and play important roles in cellular mechanotransduction processes and the regulation of various cellular functions. We recently found, in vascular smooth muscle cells (SMCs) cultured on a substrate, that the apical SFs running across the top surface of the nucleus have a mechanical connection with the cell nucleus and that their internal tension is transmitted directly to the nucleus. However, the effects of the connecting conditions and binding forces between SFs and the nucleus on force transmission processes are unclear at this stage. Here, we estimated the mechanical connection between apical SFs and the nucleus in SMCs, taking into account differences in the contractility of individual SFs, using experimental and numerical approaches. First, we classified apical SFs in SMCs according to their morphological characteristics: one subset appeared pressed onto the apical surface of the nucleus (pressed SFs), and the other appeared to be smoothly attached to the nuclear surface (attached SFs). We then dissected these SFs by laser irradiation to release the pretension, observed the dynamic behavior of the dissected SFs and the nucleus, and estimated the pretension of the SFs and the connection strength between the SFs and the nucleus by using a simple viscoelastic model. We found that pressed SFs generated greater contractile force and were more firmly connected to the nuclear surface than were attached SFs. We also observed line-like concentration of the nuclear membrane protein nesprin 1 and perinuclear DNA that was significantly located along the pressed SFs. These results indicate that the internal tension of pressed SFs is transmitted to the nucleus more efficiently than that of attached SFs, and that pressed SFs have significant roles in the regulation of the nuclear morphology and rearrangement of intranuclear DNA.

Keywords: *Cell biomechanics, Prestress, Force transmission, Laser ablation, Cytoskeleton, Mechanotransduction*

1. Introduction

Actin stress fibers (SFs) are contractile bundles of the F-actin cytoskeleton that are held together by α-actinin and contain non-muscle myosin and tropomyosin (Pellegrin and Mellor, 2007). Cells change their shape and function by assembling these SFs and exerting the contractile forces of SFs on extracellular matrices. This intracellular force transmission is critical for various biological events, including cell migration (Renkawitz et al., 2010), proliferation (Chen et al., 1997), and differentiation (Chen et al., 2007). It has recently been suggested that the nucleus is connected to the F-actin cytoskeleton by a protein complex consisting of Sad1p, UNC-84 (SUN)/Klarsicht, ANC-1, Syne homology (KASH) domain proteins, referred to as the linker of nucleus and cytoskeleton (LINC) complex (Crisp et al., 2006). This connection has been reported to play important roles in nuclear positioning during cell migration (Luxton et al., 2010; Lombardi et al., 2011) and in the mechanosensing of adherent cells (Kim et al., 2012), which may be deeply involved in intracellular force transmission from the F-actin cytoskeleton to the nucleus. From these viewpoints, we recently investigated the mechanical interaction between SFs and the nucleus in vascular smooth muscle cells (SMCs) cultured on substrates by using a laser-based nano-dissection technique (Nagayama et al., 2011; 2013): we dissected apical SFs running across the top surface of the nucleus at a point slightly outside the nucleus by laser irradiation to release fiber pretension. The fibers shortened following the dissection, and the nuclei significantly moved in the direction of shortening of the dissected fibers as if they were pulled by the contractile force of the SFs. These results indicated that apical SFs over the nucleus are connected to the nuclear surface. However, apical SFs exhibit significant morphological variation: some appear pressed onto the apical surface of the nucleus, and others appear smoothly attached to nuclear surface; the shortening of these fibers and the accompanying nuclear movements were also quite varied (Nagayama et al., 2013). The molecular components of SFs and their contractility vary with their intracellular

location (Tanner et al., 2010; Kim et al., 2012); such contractile variation may be present even among apical SFs within the same cell, and may affect contact conditions between SFs and the nucleus. Furthermore, the extent of the binding forces that may influence force transmission efficiency between SFs and the nucleus is also unclear at this stage.

In order to clarify these issues, we observed the dynamic shortening of apical SFs running across the top surface of the nucleus, and the movement of the nucleus, following laser dissection of SFs in SMCs on a substrate. Furthermore, we investigated differences in mechanical connections between SFs and the nucleus taking into account differences in SF contractility. We quantitatively estimated the pretension of SFs and the mechanical connection between SFs and the nucleus by analyzing the dynamics of SF shortening by using a simple viscoelastic model, and examined the effects of contact conditions between SFs and the nucleus on their force transmission processes.

2. Materials and Methods

2.1 Preparation of specimens

A7r5 rat embryonic aortic smooth muscle cell lines (SMCs; CRL-1444, ATCC, USA) were used as the test model. SMCs were cultured in Dulbecco's Modified Eagle's Medium (Invitrogen, Carlsbad, CA, USA) supplemented with 10% fetal bovine serum (JRH Bioscience, Lenexa, KS, USA), penicillin (100 units/ml), and streptomycin (100 µg/ml; Sigma, St. Louis, MO, USA) in a 5% CO_2 incubator at 37°C. Cells were then seeded onto glass-bottomed culture dishes (GD-0400; Ina-optica, Osaka, Japan) coated with fibronectin (100 mg/ml; Sigma, St. Louis, MO, USA), and cultured for over 24 h until they spread fully and typical SFs were developed. For fluorescence imaging, we visualized SF and nuclear DNA in living cells with GFP-actin and Hoechst 33342 (Invitrogen) using a standard protocol described elsewhere (Nagayama et al., 2011),

prior to starting the experiments.

2.2 Classification of apical SFs on the nucleus into two types

SMCs with fluorescently labeled SFs and nuclei were placed on the stage of an inverted microscope (IX71; Olympus, Tokyo, Japan) equipped with a motorized XYZ stage (ProScan H117; Prior, Jena, Germany). In this study, we obtained fluorescent image slices of apical SFs and the nucleus in the range of the thickness of the nucleus (~10 μm) at 1-μm intervals (Fig. 1) using the motorized stage, and classified these SFs running across the nuclear surface into two groups: pressed SFs (Fig. 1A–C, white arrows) and attached SFs (Fig. 1G–I). Pressed SFs appeared significantly pressed into nuclear surface, and line-like concentrations of perinuclear DNA could be observed clearly up to ~2 μm below the top surface of the nucleus (Fig. 1D–F, black arrowheads). Attached SFs appeared smoothly attached to the nuclear surface (Fig. 1G–I). Thus, we were able to distinguish the two types of apical SFs over the nucleus easily before the mechanical test. The apical SFs located away from the nucleus (non-attached SFs) were also investigated for comparison.

2.3 Observation of SFs and nuclei during laser nano-dissection of single SFs

SMCs were placed on the microscope stage, and the experiment environment was maintained similar to that in a CO_2 incubator (Nagayama et al., 2011). The microscope was combined with laboratory-built laser nanoscissor equipped with an ultraviolet pulsed laser, with wavelength and pulse width of 355 nm and ~400 ps, respectively (FTSS355-Q1; CryLaS GmbH, Berlin, Germany). First, we obtained whole-cell images of target cells to measure the length of SFs. Then, we carefully confirmed the focus position of the target SFs located over the nucleus using the motorized Z-stage. The laser beam was focused onto the target fibers using a 100× oil-immersion objective lens (NA = 1.4), and a single SF was cut by laser irradiation for 1 s. The irradiation point

on the target SF was ~10 μm away from the outline of nucleus to prevent the disruption of the nuclear membrane. Subsequently, we captured the resultant shortening of the dissected SF and the movement of the nucleus with an electron-multiplying CCD camera (C9100-12; Hamamatsu Photonics, Hamamatsu, Japan) for 5 min. Using these captured images, we traced the trajectory of shortening of the dissected fibers to measure their shortening ratio. We also measured the change in the position of the nuclear centroid following SF dissection.

2.4 Observation of nuclear morphology using confocal microscopy

To confirm the contact conditions between apical SFs and nucleus in detail, we obtained confocal fluorescence image slices of the SFs, nucleus, and nuclear membrane protein nesprin 1, which tethers the outer nuclear membrane to the F-actin cytoskeleton (Warren et al., 2005; Crisp et al., 2006), in the range of the thickness of the nucleus (~10 μm) at 0.25-μm intervals, using a confocal system (CSU-X1; Yokogawa, Tokyo, Japan) with a multicolor fluorescence system (Light Engine Spectra-X, Optline, Tokyo, Japan). Prior to observation, the cells were fixed and permeabilized, and SFs in the cells were stained by incubating with Alexa Fluor 488-conjugated phalloidin (Molecular Probes) at a concentration of ~200 nM for 30 min. Nuclei were also stained with Hoechst 33342 as described in *Section 2.1*. For nesprin 1 staining, the cells were incubated for 1 h at room temperature with a polyclonal primary antibody against nesprin 1 (1:50 dilution; Syne-1 [H-100], sc-99065; Santa Cruz Biotechnology, Santa Cruz, CA, USA) in PBS containing 1% bovine serum albumin (Sigma, St. Louis, MO, USA). After washing, cells were incubated for 30 min at room temperature with an Alexa Fluor 546-conjugated secondary antibody (1:200 dilution; Molecular Probes, Carlsbad, CA).

2.5 Data analysis

Data were expressed as mean ± SD. Statistically significant differences in the

shortening of SFs and nuclear displacement were assessed by unpaired Student's *t*-test. The estimated mechanical parameters of SFs were analyzed using ANOVA with a correction for multiple comparisons, followed by a Steel-Dwass multiple comparison of the means between two groups using a statistical analysis program (MEPHAS, http://www.gen-info.osaka-u.ac.jp/MEPHAS/). *P* values <0.05 were considered significant for all analyses.

3. Results and Discussion

Thick SFs running across the apical surface of the nucleus were clearly observed in SMCs (Fig. 2). A line-like concentration of perinuclear DNA was observed underneath the pressed SFs (Fig. 2E, red arrowhead). Following SF dissection with laser irradiation, the pressed SFs shortened across the top surface of the nucleus (Fig. 2A–D), and their shortening displacement reached over 70% within 5 min (Fig. 3A, red triangular symbols). Nuclei also moved significantly after the dissection of the pressed SFs, as if they were being pulled by the contractile force of the dissected fibers. Some nuclei showed marked local deformation beneath the dissected fibers (Fig. 2F–H), and the internuclear DNA looked condensed at such locations (Fig. 2H, white arrow). On the other hand, the shortening of the attached SFs after dissection was significantly smaller than that of the pressed SFs (Fig. 2I–L and Fig. 3A, blue circular symbols), and the nuclei did not show marked deformation (Fig. 2M–P). A statistically significant difference in the shortening ratios of the two types of SFs was already observed at 1 min after dissection (Fig. 3A). The shortening of the pressed and attached SFs reached a plateau more slowly than the apical SFs located away from the nucleus (non-attached SFs: Fig. 3A, open square symbols).

From the dynamics of SF shortening, we estimated the pretension of these two types of apical SFs and the mechanical connection between these fibers and the nucleus. The

trajectory of the shortening of SFs crossing the top surface of the nucleus could be predicted by a viscoelastic model based on a Kelvin-Voigt model with a parallel combination of a spring and dashpots (Fig. 3B). In this model, we simply assumed that apical SFs running across the apical surface of the nucleus were viscoelastic fibers with a spring constant, k_{SF}, a viscosity, η_{SF}, and strain, $\varepsilon_{SF}(t)$, and that they were attached to the substrate only at the two ends via focal adhesions. The stiffness of single SFs of SMCs has been reported to be ~0.5 nN/% strain, as obtained from the tensile test of isolated SFs (Deguchi et al., 2005; 2006) and isolated SMCs (Nagayama and Matsumoto, 2010); thus, we used this value as the spring constant (k_{SF}) of SFs in SMCs for analysis. The shortening ratio of the dissected SFs, $\Delta\varepsilon_{SF}(t)$, is represented as the difference between the prestrain, $\varepsilon_{SF}(0)$, and the strain at time t, $\varepsilon_{SF}(t)$, as given by $\Delta\varepsilon(t) = (\varepsilon_{SF}(0) - \varepsilon_{SF}(t))/(\varepsilon_{SF}(0)+1)$. The dissected end of the SF is subjected to an opposing viscous resistance force from its fiber viscosity $\eta_{SF}\cdot(d\varepsilon_{SF}(t)/dt)$ where η_{SF} represents the viscosity of SF itself. In this study, the average displacement of the nucleus was less than 1/7 that of the dissected SFs (Fig. 2). Furthermore, large differences were observed between the time constant of the non-attached apical SFs and those of the attached and the pressed SFs (Fig. 3). These results indicate that resistant forces acting on the pressed and attached SFs during their shortening are mainly due to the viscous resistance between these SFs and nuclear surface. Thus we assumed that the dissected SF is also subjected to an opposing viscous resistance force from the stationary nuclear surface $\eta_{SF\text{-}Nuc}\cdot(d\varepsilon_{SF}(t)/dt)$, where $\eta_{SF\text{-}Nuc}$ represents the viscosity subjected to the connection between SFs and nuclear surface. Thus, the force $F(t)$ acting on the dissected end of the SF is represented as $F(t) = k_{SF}\cdot\varepsilon_{SF}(t) - (\eta_{SF} + \eta_{SF\text{-}Nuc})\cdot(d\varepsilon_{SF}(t)/dt)$, and the force at $t = 0$ is equal to the SF pretension, F_{pre}, just before dissection (Fig. 3B). Using this model, the time-dependent change in the shortening ratio of SFs, $\Delta\varepsilon(t)$, was fitted satisfactorily in all the SF shortening data (Fig. 3A, $R^2 > 0.99$). We analyzed the change in the shortening ratio of the non-attached SFs and obtained their viscosity

(Table 1). Then we used this average value as a viscosity of SF itself (η_{SF} = 17 nN/%·s) and consequently obtained the estimated value of SF pretension, F_{pre}, and the viscosity, $\eta_{SF\text{-}Nuc}$, which was dependent on the connection strength between SFs and the nuclear surface (Table 1). The estimated value of F_{pre} was 15 ± 2 nN (n = 10, mean ± SD) in the non-attached SFs, 61 ± 23 nN (n = 14) in the pressed SFs, and 21 ± 10 nN (n = 11) in the attached SFs; these are in the same order of magnitude as the traction force at each focal adhesion in SMCs measured using the elastic micropillar substrate (Nagayama and Matsumoto, 2011). The time constant of shortening of the non-attached apical SFs was 34 ± 13 s (n = 10, mean ± SD), which was significantly larger than that of the basal SFs in endothelial cells (less than 20 s) reported by Kumar et al. (2006). This difference may be due to the different intracellular locations occupied by the SFs (apical side or basal side); the retraction of the basal SFs was restricted to the proximity of the dissection point, indicating that the basal SFs were attached to the substrate at various adhesion sites (Colombelli et al., 2009; Nagayama et al., 2013). In contrast, the apical SFs were attached to the substrate only at both ends with focal adhesions.

Both F_{pre} and $\eta_{SF\text{-}Nuc}$ were over two-fold larger in pressed SFs than in attached and non-attached SFs, indicating that pressed SFs have higher contractility compared to other SFs, and that pressed SFs connect more firmly to the apical surface of the nucleus. Such strong connections produced large viscous resistance forces acting on the nuclear surface and significant movement of the nucleus in the direction of SF shortening following the dissection of pressed SFs (Fig, 4A, D), compared to that seen with attached SFs (Fig. 4B, D), even though the lateral motion of the nucleus was quite small following the dissection of both types of SFs (Fig. 4E). Recent studies suggest that the contractility of SFs vary with their intracellular location, such as the apical or basal side of cells (Kim et al., 2012; Nagayama et al., 2013), and the cell center or cell periphery (Tanner et al., 2010), and that these differences depend on the variability of myosin light chain phosphorylation in individual SFs (Kim et al., 2012). These reports and the

results of this study indicate that pressed SFs over the nucleus might contain more activated myosin II than attached SFs, and there is great contractile variability even among apical SFs over the nucleus, although the reason for this variability in SMCs is still unclear.

In order to further understand the mechanical connection between SFs and the nucleus, we observed the three-dimensional localization of the LINC complex protein nesprin 1, which tethers the outer nuclear membrane to the F-actin cytoskeleton, and the localization of internuclear DNA, and analyzed their distribution with reference to the localization of SFs on the apical side of the nucleus. We observed the line-like concentration of nesprin 1 located along the pressed SFs (Fig. 5B, white arrowheads; Fig. 5I, upper panel). In this arrangement, the nuclear surface was significantly compressed vertically by the pressed SFs (Fig. 5C, inset) and a linear concentration of perinuclear DNA was aligned in the direction of the pressed SFs (Fig. 5I, lower panel). In contrast, the distribution of nesprin 1 tended to be sparse at the apical surface of the nucleus, which contains attached SFs (Fig. 5F; Fig. 5J, upper panel), and the apical surface of the nucleus looked smooth (Fig. 5G, inset). We also confirmed that the linear concentrations of perinuclear DNA aligned with the pressed SFs were induced with increasing contractile force of SFs by blocking myosin light chain dephosphorylation, and consequently increased the proportions of the cells showing linear DNA concentration (Fig. 6). These results strongly suggest that pressed SFs compress the nuclear surface physically and that they are firmly connected to the nuclear surface with abundant nuclear membrane proteins. These connections between SFs and the nucleus were tension-dependent. The contractile force of a single SF significantly affected not only the stabilization of nuclear position but also nuclear morphology and the distribution of internuclear DNA. Recent studies have demonstrated that nuclear morphology affects many cellular functions, such as cell migration (Gerlitz et al., 2011), cell mitosis (Minc, N et al., 2011), and cell differentiation (Rozwadowska et al., 2013). Thus, the

mechanical connection between SFs and the nucleus observed in this study may play prominent roles in controlling these cellular functions.

In conclusion, we have estimated for the first time the mechanical connection between the apical SFs and the nucleus in SMCs, taking into account differences in the contractility of individual SFs, by using experimental and numerical approaches. We found that apical SFs that appear pressed into the nuclear surface generated greater contractile force and were more firmly connected to the nuclear surface via LINC complex proteins. Such fibers may have significant roles in the regulation of nuclear morphology and rearrangements of intranuclear DNA. Further studies are ongoing in our laboratory to confirm this notion.

Conflict of interest statement: The authors declare that they have no conflict of interest with regard to this manuscript.

Acknowledgements

This work was supported in part by MEXT and JSPS KAKENHIs (nos. 24680051, 24650257, and 25111711 to K.N., and no. 22127008 and 22240055 to T.M.), and the Hibi Science Foundation, Japan (K.N.).

REFERENCES

1. Chen, C.S., Mrksich, M., Huang, S., Whitesides, G.M., and Ingber, D.E., 1997. Geometric control of cell life and death. *Science* 276, 1425–1428.
2. Chen J, Li H, SundarRaj N, Wang JH. 2007. Alpha-smooth muscle actin expression enhances cell traction force. *Cell Motil Cytoskeleton*. 64(4), 248-257.
3. Colombelli, J., Besser, A., Kress, H., Reynaud, E.G., Girard, P., Caussinus, E., Haselmann, U., Small, J.V., Schwarz, U.S., and Stelzer, E.H., 2009. Mechanosensing in actin stress fibers revealed by a close correlation between force and protein localization. *J. Cell Sci.* 122(Pt 10), 1665-1679.
4. Crisp M., Liu, Q., Roux, K., Rattner, J.B., Shanahan, C., Burke, B., Stahl, P.D., Hodzic, D., 2006. Coupling of the nucleus and cytoplasm: role of the LINC complex, *J. Cell Biol.* 172, 41–53.
5. Deguchi, S., Ohashi, T., Sato, M., 2005. Newly designed tensile test system for in vitro measurement of mechanical properties of cytoskeletal filaments, JSME int. J. Ser. C, 48(4), 396-402.
6. Deguchi, S., Ohashi, T., and Sato, M., 2006. Tensile properties of single stress fibers isolated from cultured vascular smooth muscle cells, *J Biomech.* 39(14), 2603-2610.
7. Gerlitz, G., and Bustin, M. (2011), The role of chromatin structure in cell migration. T*rends Cell Biol.* 21-1, 6-11.
8. Kim, D.H., Khatau, S.B., Feng, Y., Walcott, S., Sun, S.X., Longmore, G.D., Wirtz, D., 2012. Actin cap associated focal adhesions and their distinct role in cellular mechanosensing, *Sci Rep.* 2, 555, doi: 10.1038/srep00555.
9. Kumar, S., Maxwell, I.Z., Heisterkamp, A., Polte, T.R., Lele, T.P., Salanga, M., Mazur, E., and Ingber, D.E., 2006. Viscoelastic retraction of single living stress fibers and its impact on cell shape, cytoskeletal organization, and extracellular matrix mechanics. *Biophys J.* 90(10), 3762-3773.
10. Lombardi ML, Jaalouk DE, Shanahan CM, Burke B, Roux KJ, Lammerding J., 2011.

The interaction between nesprins and sun proteins at the nuclear envelope is critical for force transmission between the nucleus and cytoskeleton. *J Biol Chem*. 286(30), 26743-26753.

11. Luxton, G.W., Gomes, E.R., Folker, E.S., Vintinner, E., and Gundersen, G.G., 2010. Linear arrays of nuclear envelope proteins harness retrograde actin flow for nuclear movement. *Science*. 329(5994), 956-959.
12. Minc, N., Burgess, D., and Chang, F., 2011. Influence of cell geometry on division-plane positionin. *Cell* 144-3, 414-426.
13. Nagayama, K., and Matsumoto, T., 2010. estimation of single stress fiber stiffness in cultured aortic smooth muscle cells under relaxed and contracted states: its relation to dynamic rearrangement of stress fibers, *J Biomech*. 43, 1443-1449.
14. Nagayama, K., and Matsumoto, T., 2011. Dynamic change in morphology and traction forces at focal adhesions in cultured vascular smooth muscle cells during contraction, *Cell. Mol. Bioeng*. 4-3, 348-357.
15. Nagayama, K., Yahiro, Y., and Matsumoto, T., 2011. Stress fibers stabilize the position of intranuclear DNA through mechanical connection with the nucleus in vascular smooth muscle cells. *FEBS Letters* 585-24, 3992-3997.
16. Nagayama, K., Yahiro, Y., and Matsumoto, T., 2013. Apical and basal stress fibers have different roles in mechanical regulation of the nucleus in smooth muscle cells cultured on a substrate. *Cell. Mol. Bioeng*. 6-4, 473-481.
17. Pellegrin S, Mellor H., 2007. Actin stress fibres. *J Cell Sci.* 120(Pt 20), 3491-3499.
18. Renkawitz, J., Sixt, M., 2010, Mechanisms of force generation and force transmission during interstitial leukocyte migration, *EMBO Rep*. 11, 744–750.
19. Rozwadowska N, Kolanowski T, Wiland E, Siatkowski M, Pawlak P, Malcher A, Mietkiewski T, Olszewska M, Kurpisz M., 2013. Characterisation of nuclear architectural alterations during in vitro differentiation of human stem cells of myogenic origin. *PLoS One*. 8(9), e73231. doi: 10.1371/journal.pone.0073231.

20. Tanner, K., Boudreau, A., Bissell, M.J., and Kumar, S., 2010. Dissecting regional variations in stress fiber mechanics in living cells with laser nanosurgery. *Biophys J.* 99(9), 2775-2783.

21. Warren, D.T., Zhang, Q., Weissberg, P.L., Shanahan, C.M., 2005. Nesprins: intracellular scaffolds that maintain cell architecture and coordinate cell function?, *Expert Rev Mol. Med.* 7, 1–15.

FIGURE LEGENDS

Figure 1

Typical examples of fluorescence images of apical SFs and the nucleus in living SMCs. To visualize the cell nucleus, nuclear DNA was stained with Hoechst 33342 (Molecular Probes). The cells were classified into two types: one had line-like concentrations of intranuclear DNA along the apical SFs (pressed SFs: D–F, black arrowheads), and the other did not have such concentrations of intranuclear DNA (attached SFs: J–K). Bar = 10 μm.

Figure 2

Fluorescent images of SFs and the nucleus during laser nano-dissection of pressed SFs (A–H) and attached SFs (I–P). The black crosses in A and I represent the irradiation points of the laser beam. White arrowheads indicate one of the dissected ends of the SFs. Scale bars = 10 μm.

Figure 3

Changes in the shortening ratio of SFs following laser dissection (A). The viscoelastic model based on Kelvin-Voigt model was used to analyze the dynamics of SF shortening across the apical surface of the nucleus (B). k_{SF}, spring constant of SFs; η_{SF}, viscosity of SFs; $\eta_{SF\text{-}Nuc}$, viscosity subjected to the connection between SFs and nuclear surface; $F(t)$, force acting on the dissected end of the SFs; F_{pre}, pretension of the dissected SFs; $\varepsilon_{SF}(t)$, strain of the dissected SFs; $\varepsilon_{SF}(0)$, prestrain of the dissected SFs; $\Delta\varepsilon_{SF}(t)$, shortening ratio of the dissected SFs; τ, time constant of the shortening of the dissected SFs. The thin curves in (A) correspond to the predicted shortening using the model described in (B). Model parameters were determined by minimizing errors between the theoretical and experimental curves within the range $0 \leq t \leq 300$ s using a Microsoft Excel Visual Basic for Applications (VBA) macro (Microsoft).

Figure 4

The trajectory of movement of the nuclear centroid following laser nano-dissection of pressed SFs (A) and attached SFs (B) with reference to the shortening direction (X direction) of the dissected SFs. The direction of movement of the nucleus is defined in (C). The maximum displacement of the nucleus in the X (D) and Y (E) direction was compared between the dissection of pressed and attached SFs. Occasionally, the direction of nuclear movement following SF dissection suddenly changed to backward direction at a later stage of movement (A and B, #).

Figure 5

Typical examples of fluorescent confocal images of apical SFs (A, E), nesprin 1 (B, F), intranuclear DNA (C, G), and their merged image (D, H) in SMCs showing pressed (A–D) or attached SFs (E–H). Bars = 10 μm. Fluorescence intensity distribution of SFs, nesprin 1, and DNA in the dashed lines in D and H is shown in I and J, respectively. Note that the significant intensity peaks of nesprin 1 and DNA are located at the peaks of the pressed SFs (I, black arrows) but not at those of the attached SFs (J).

Figure 6

A typical example of fluorescence images of apical SFs and the nucleus in SMCs before (A, B) and after (C, D) the contraction of SFs with calyculin-A treatment (10 nM, 20 min), which inhibits myosin light chain phosphatase, thereby increasing myosin light chain phosphorylation. Bars = 50 μm. Arrowheads in D represent the linear concentrations of perinuclear DNA aligned along the apical SFs (DNA line). Note that the higher magnification of nuclei in the dashed rectangle areas in D show some indentations at their outlines (E and F, arrows). The frequency of cells showing the DNA line was calculated and compared between untreated cells and cells treated with calyculin-A (G). In panel (G), over 300 cells were analyzed for each condition.

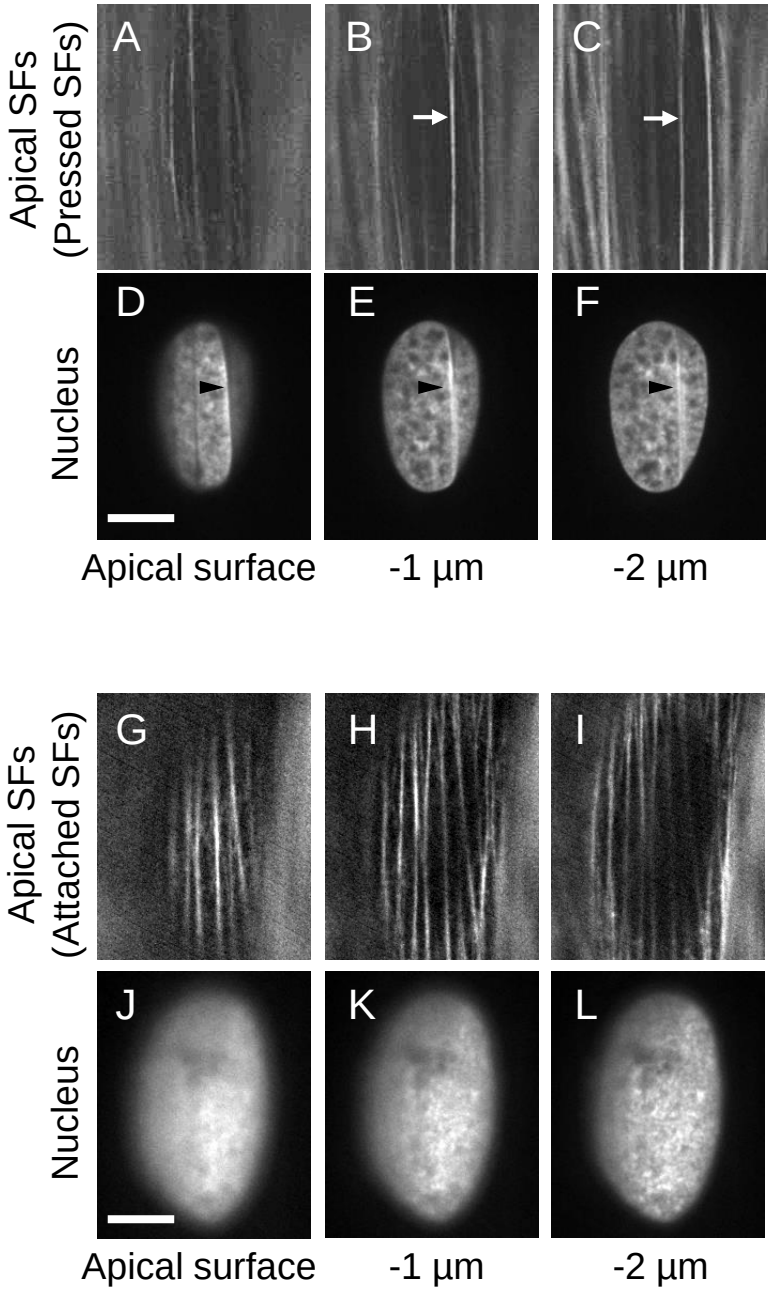
Apical SFs
(Pressed SFs)
A
B
C
Nucleus
D
E
F
Apical surface
-1 μm
-2 μm
Apical SFs
(Attached SFs)
G
H
I
Nucleus
J
K
L
Apical surface
-1 μm
-2 μm

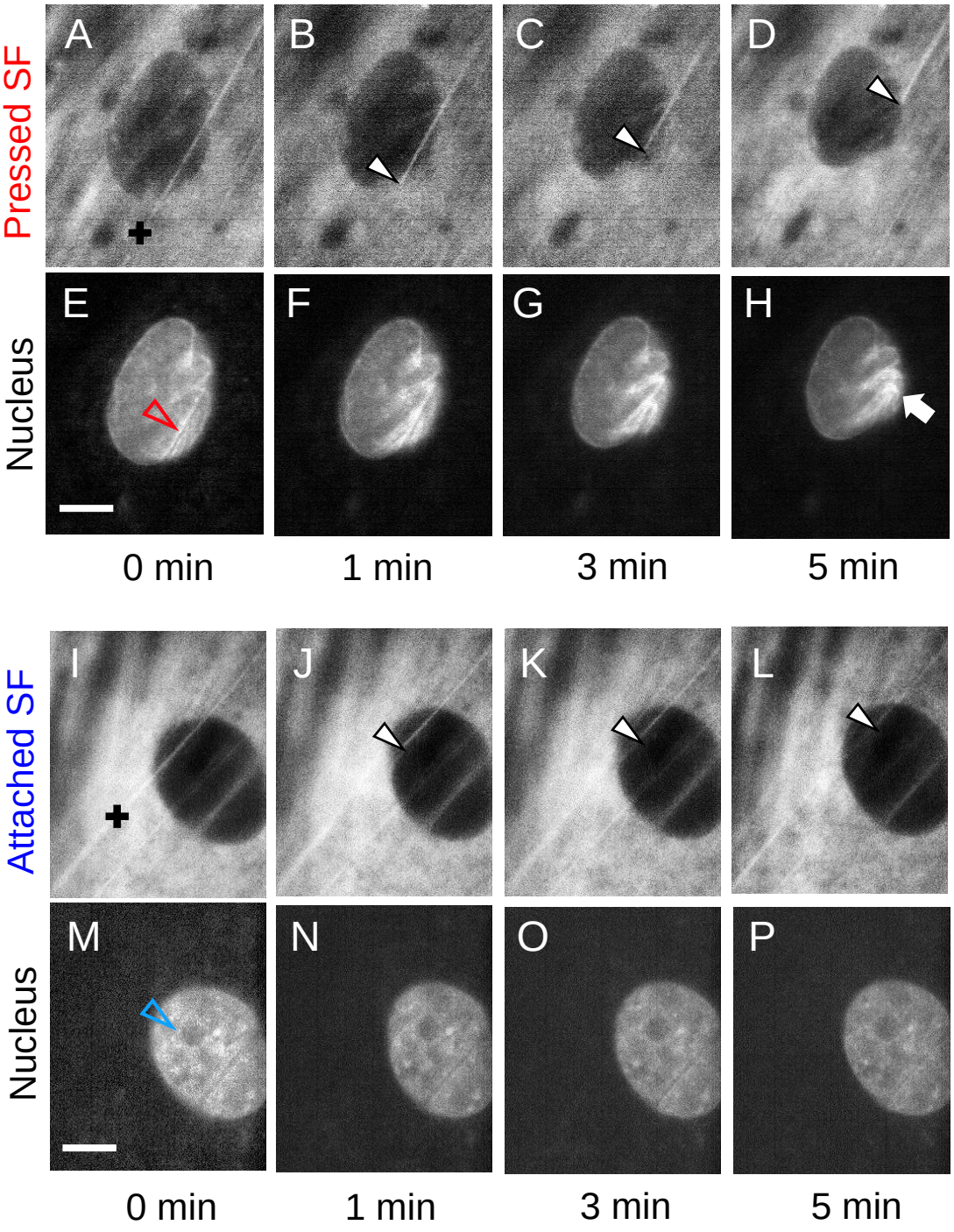
Pressed SF
A
B
C
D
Nucleus
E
F
G
H
0 min
1 min
3 min
5 min
Attached SF
I
J
K
L
Nucleus
M
N
O
P
0 min
1 min
3 min
5 min

A

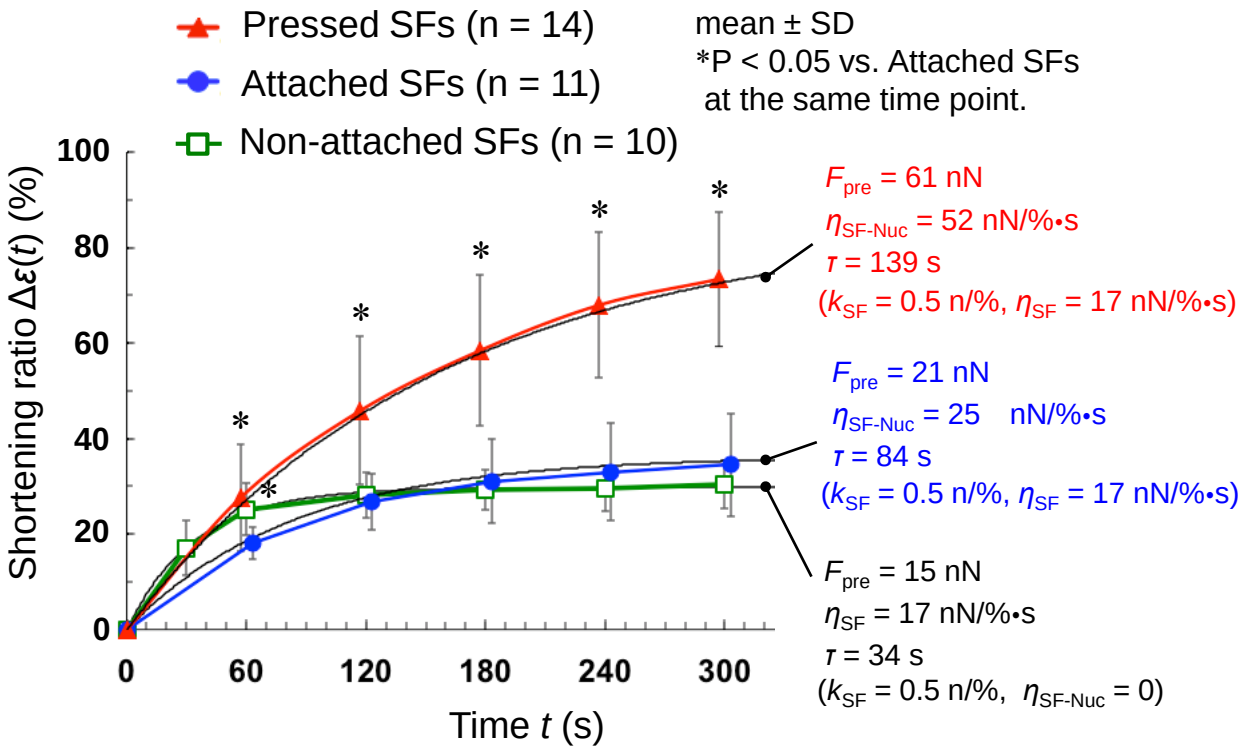

B

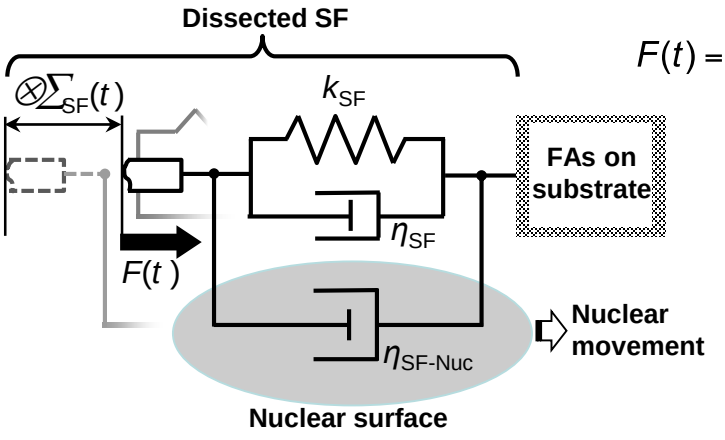

$$F(t) = k_{SF} \cdot \varepsilon_{SF}(t) - \left(\eta_{SF} + \eta_{SF-Nuc}\right) \cdot \frac{d\varepsilon_{SF}(t)}{dt}$$

$$De_{SF}(t) = \frac{e_{SF}(0) - e_{SF}(t)}{e_{SF}(0) + 1}$$

$$F(0) = F_{pre}$$

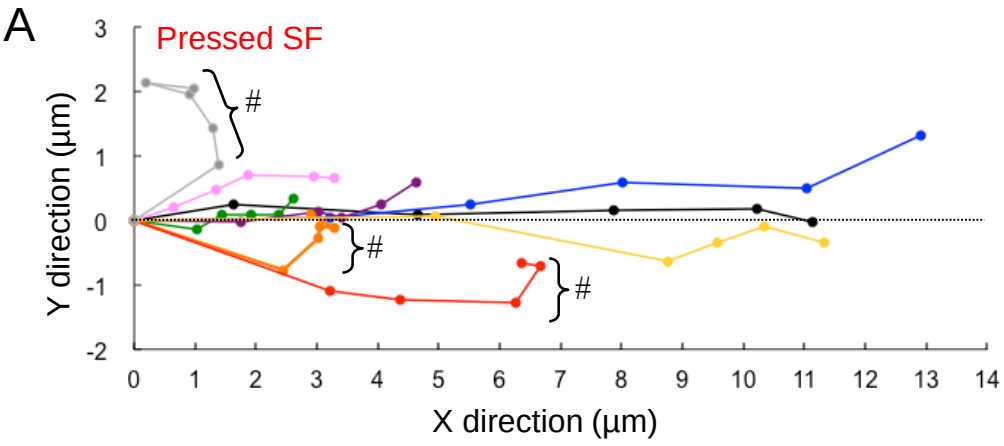
A
Pressed SF
Y direction (μm)
X direction (μm)
#
#
#

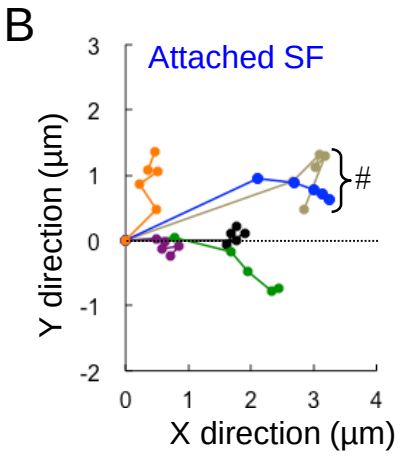
B
Attached SF
Y direction (μm)
X direction (μm)
#

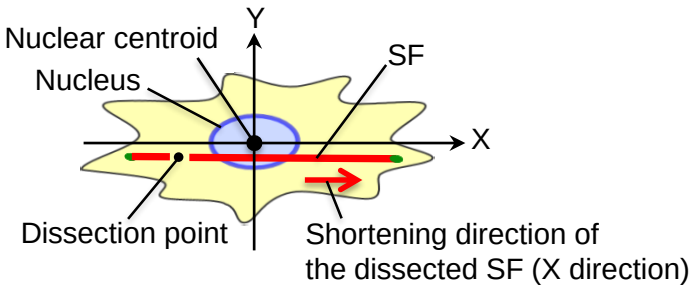
C
Nuclear centroid
Nucleus
Y
SF
X
Dissection point
Shortening direction of
the dissected SF (X direction)

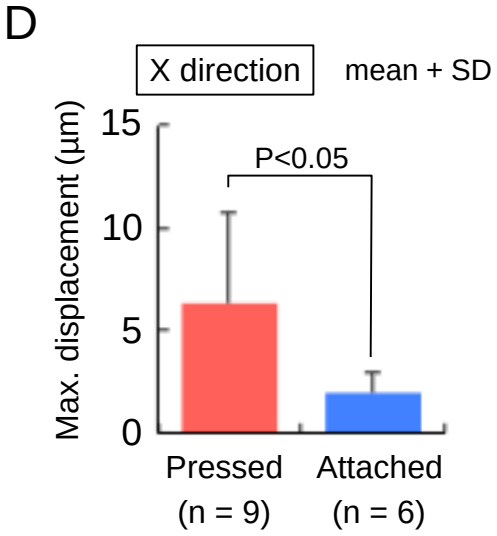
D
X direction
mean + SD
Max. displacement (μm)
P<0.05
Pressed
(n = 9)
Attached
(n = 6)

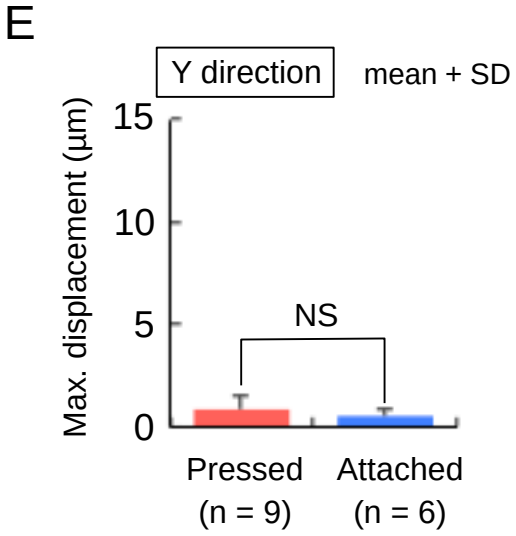
E
Y direction
mean + SD
Max. displacement (μm)
NS
Pressed
(n = 9)
Attached
(n = 6)

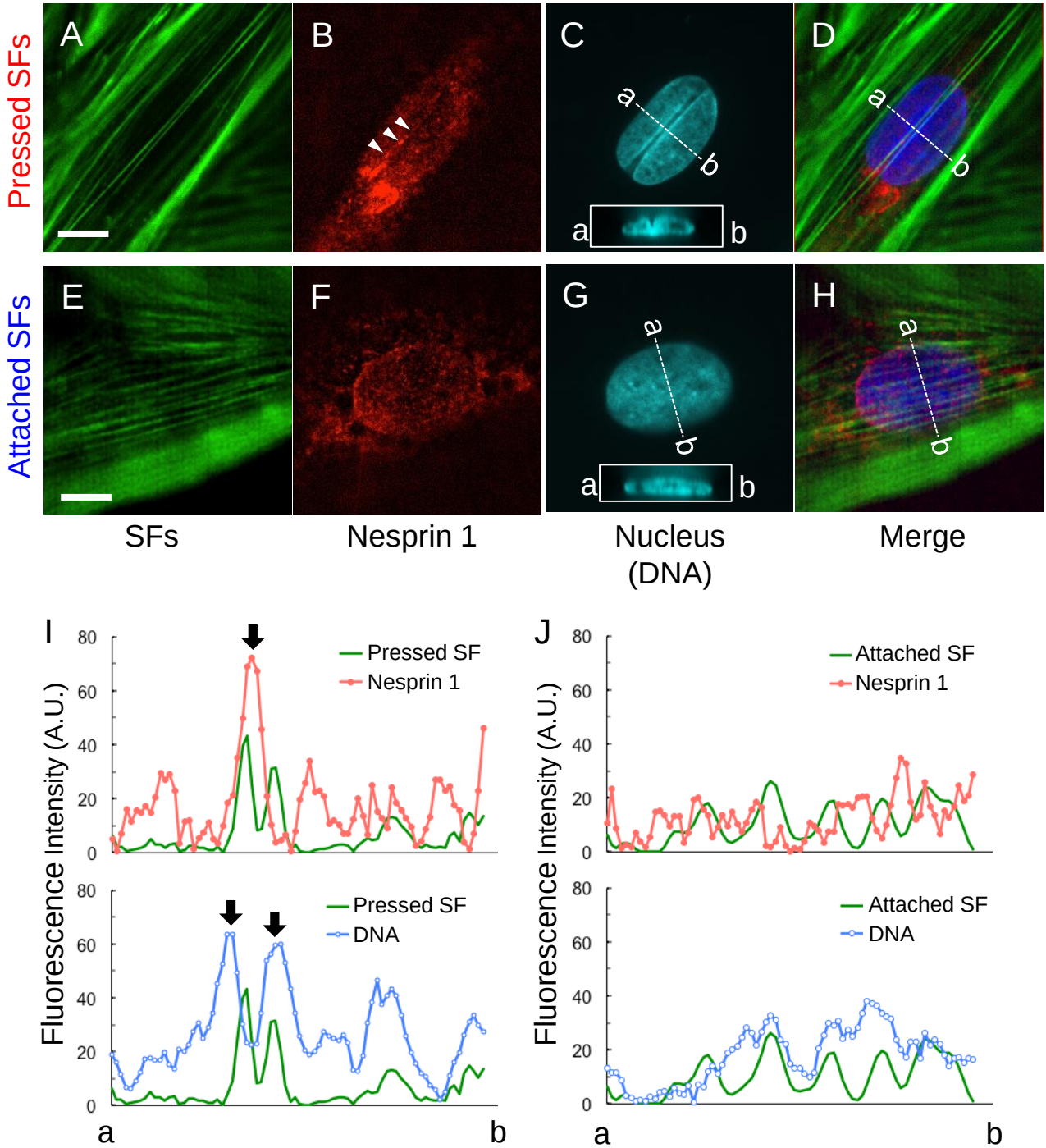
Pressed SFs
Attached SFs
A
B
C
D
E
F
G
H
a
b
SFs
Nesprin 1
Nucleus (DNA)
Merge
I
J
Fluorescence Intensity (A.U.)
Pressed SF
Nesprin 1
DNA
Attached SF
0
20
40
60
80

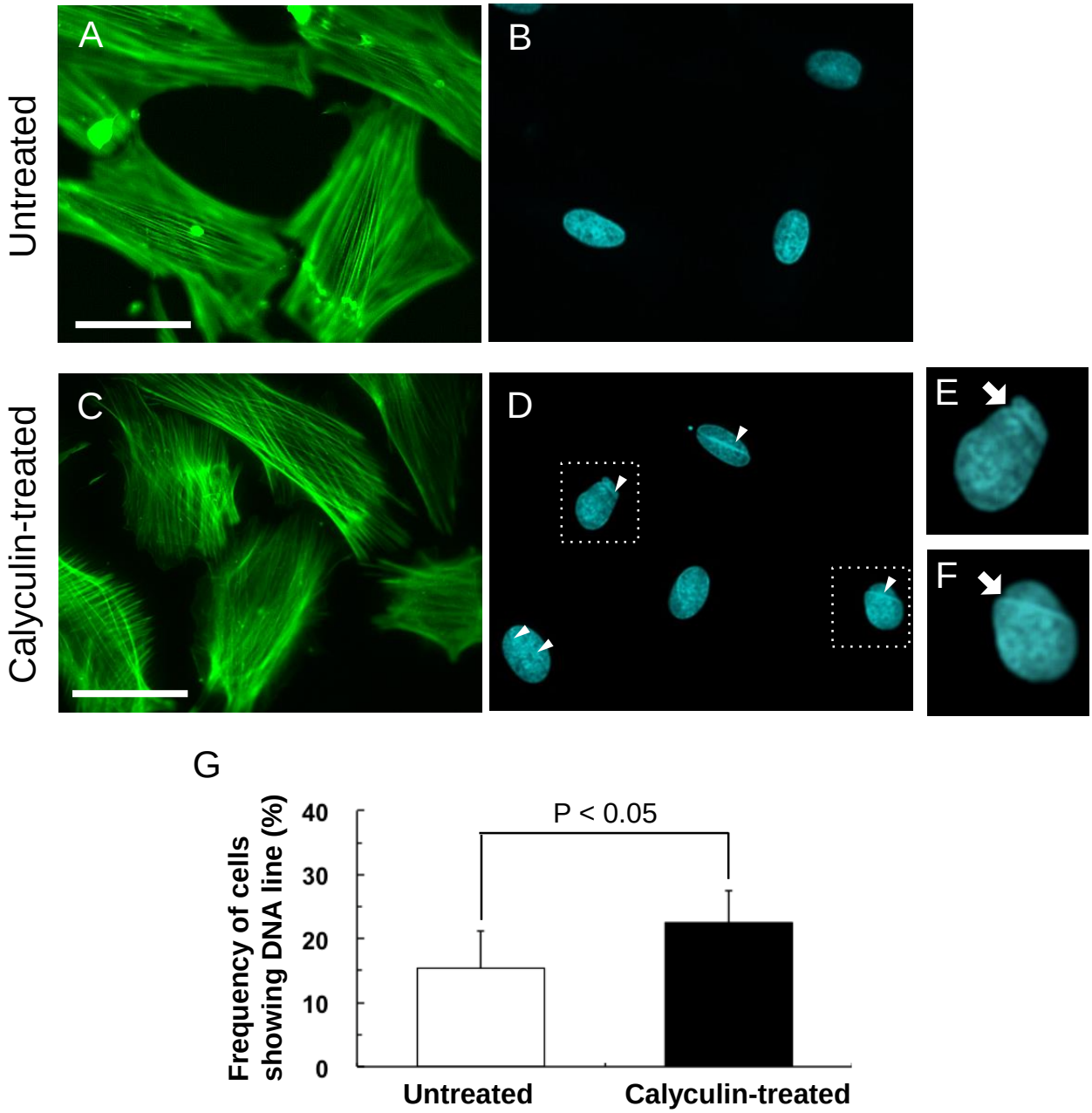
Untreated
Calyculin-treated
A
B
C
D
E
F
G
Frequency of cells showing DNA line (%)
40
30
20
10
0
P < 0.05
Untreated
Calyculin-treated

Table 1 Summary of the pretension of the pressed and attached SFs runnnig across the top surface of the nucleus and mechanical interaction between them. The pretension and viscosity of apical SFs located away from the nucleus (non-attached SFs) are also shown for comparison. (mean ± SD)

Specimens	n	F_{pre} (nN)	η_{SF} (nN/% · s)	$\eta_{SF\text{-}Nuc}$ (nN/% · s)	τ (s)
Non-attached SFs	10	15 ± 2	17 ± 6	–	34 ± 13
Pressed SFs	14	61 ± 23$^{\#}$] *	(17)	52 ± 34] *	139 ± 67$^{\#}$] *
Attached SFs	11	21 ± 10] *	(17)	25 ± 16] *	84 ± 36$^{\#}$] *

F_{pre}, pretension of SFs before their dissection; η_{SF}, viscosity of apical SFs located away from the nucleus; $\eta_{SF\text{-}Nuc}$, viscosity acting between the dissected SFs and the nuclear surface; τ, time constant of the shortening of the dissected SFs; *P < 0.05; $^{\#}$P < 0.05 vs. non-attached SFs.